Article

Discovery Medicine 2025; 37(201): 2360–2370
https://doi.org/10.24976/Discov.Med.202537201.200

Forkhead Box Protein 1 Protects the Glycocalyx and Mitigates COPD by Suppressing MMP9

Fan Zhou[1,*], Yajie Shi[2], Yu Wang[1], Xiaolong He[1]

[1]Department of Cardiovascular Diseases, Hangzhou TCM Hospital Affiliated to Zhejiang Chinese Medical University, 310007 Hangzhou, Zhejiang, China
[2]Department of Respiratory and Critical Care Medicine, Hangzhou TCM Hospital Affiliated to Zhejiang Chinese Medical University, 310007 Hangzhou, Zhejiang, China
*Correspondence: Zfzhoufanzf@163.com (Fan Zhou)
Submitted: 21 August 2025 Revised: 1 September 2025 Accepted: 15 September 2025 Published: 20 October 2025

Background: Smoking-induced glycocalyx significantly contributes to the pathogenesis of chronic obstructive pulmonary disease (COPD). Forkhead box protein 1 (Foxp1) reduces the expression of matrix metalloproteinase 9 (MMP9), thereby preventing glycocalyx injury. Therefore, we hypothesized that Foxp1 may maintain the integrity of the glycocalyx by inhibiting MMP9, thereby alleviating COPD.

Methods: We established COPD mouse models and intervened with Adeno-associated virus 9 (AAV9)-Foxp1. The mean linear intercept (MLI) and apoptosis of the lung tissue were analyzed using histological staining. Human pulmonary microvascular endothelial cells (hPMVECs) were transfected with Foxp1 plasmid and or MMP9 plasmid and then exposed to cigarette smoke extract (CSE) to establish *in vitro* cellular model. The expressions of glycocalyx-related proteins (Versican, syndecan-1 and MMP9) and Foxp1 were assessed using Western blotting and quantitative reverse transcription polymerase chain reaction (qRT-PCR) analysis. Cellular viability, apoptosis, endothelial permeability, and tube formation capabilities were determined using the cell counting kit-8 (CCK-8) assay, flow cytometry, transwell assay, and tube formation assay, respectively.

Results: *In vivo*, AAV9-Foxp1 treatment significantly reduced MLI and endothelial apoptosis in COPD mice ($p < 0.05$). It also suppressed MMP9 expression while increasing Versican and syndecan-1 levels, indicating glycocalyx protection ($p < 0.05$). *In vitro*, Foxp1 overexpression counteracted CSE-induced damage by enhancing cell viability, reducing apoptosis, improving endothelial barrier function, and promoting tube formation ($p < 0.05$). Furthermore, Foxp1 upregulation restored glycocalyx integrity by increasing syndecan-1 and decreasing MMP9 expression. However, these protective effects were abolished when MMP9 was overexpressed simultaneously, confirming that Foxp1 acts through the inhibition of MMP9 ($p < 0.05$).

Conclusion: Foxp1 protects glycocalyx from injury to relieve COPD by downregulating MMP9, highlighting its potential as a promising therapeutic target.

Keywords: chronic obstructive pulmonary disease; glycocalyx; forkhead box protein 1; matrix metalloproteinase 9

Introduction

Chronic obstructive pulmonary disease (COPD) is a progressive respiratory disease characterized by persistent respiratory symptoms and is a leading cause of death worldwide, with its prevalence increasing annually [1]. The hallmark pathological feature of COPD is emphysema, which involves damage to lung tissue and enlargement of the alveoli, leading to impaired oxygen exchange and ultimately dyspnea. While progression of COPD can be prevented by reducing exposure to risk factors such as tobacco smoke, current therapeutic approaches primarily focus on symptom management using bronchodilators and anti-inflammatory agents [2]. Despite these management strategies, COPD remains a severe public health concern due to difficulties in early diagnosis, limited therapeutic options, and likelihood of disease progression [3]. Therefore, it is crucial to explore the underlying pathogenesis of COPD and develop novel therapeutic strategies.

Endothelial cells play a pivotal role in the pathogenesis of COPD-associated emphysema. Loss and apoptosis of endothelial cells are typical features of COPD, and the recovery of these cells has been reported to reverse emphysematous alterations [4]. Notably, the endothelial glycocalyx, a polysaccharide-protein complex covering the surface of vascular endothelial cells, offers vascular protection and is critical for regulating vascular permeability, inflammatory responses, and shear stress stability [5]. However, various factors such as smoking, oxidative stress, and trauma can result in degradation or shedding of the glycocalyx, disrupting its protective functions, and leading to increased vascular permeability and decreased vascular tension [6]. Tian Jiang *et al*. [7] reported that preventing glycocalyx injury and endothelial cell apoptosis can alleviate COPD progres-

sion. These observations suggest that maintaining the integrity of the glycocalyx may represent a novel approach for the treatment of COPD.

The forkhead box protein 1 (*Foxp1*) gene is highly expressed in vascular endothelial cells and can inhibit the expression of matrix metalloproteinase 9 (MMP9) [8], a key enzyme involved in the degradation of glycocalyx [9]. Moreover, the Foxp1 gene is implicated in the regulation of lung development and lung function. Silencing of Foxp1 in lung epithelial cells has been reported to upregulate the expression of MMPs and inflammatory factors in response to cigarette smoke extract (CSE), indicating a protective role of Foxp1 in tobacco-related lung diseases [10]. Based on these observations, we assume that *Foxp1* may protect the endothelial glycocalyx and reduce COPD by downregulating MMP9.

Materials and Methods

Experimental Animals

Male C57BL/6J mice (n = 24), weighing 20–23 g and aged 6–8 week, were obtained from Hangzhou Medical College (China), and were housed under specific pathogen-free (SPF) conditions with a 12-hour light/dark cycle, a temperature of 22 ± 2 °C, a humidity of 50 ± 10%, and had free access to food and water. All experimental procedures involving animals were approved by the Institutional Animal Care and Use Committee, Zhejiang Center of Laboratory Animals (ZJCA) (ZJCLA-IACUC-20011026).

Mice were randomly divided into four groups (n = 6 per group): control (Con), COPD, adeno-associated virus 9 (AAV9)-vector, and AAV9-Foxp1. The COPD model was established as previously described [7]. Briefly, mice were placed in a smoking exposure chamber (PAB-S200, Beijing Biolaunching Technologies Co., Ltd., Beijing, China) and exposed to smoke from 10 filter-tip cigarettes twice a day, five days per week, over a period of three months. The primary airflow was maintained at 1.0 L/minute, and the dilution airflow was 6.0 L/minute. Each smoke exposure lasted for 1 hour, with a minimum interval of 4 hours between exposures. Mice in the Con group were exposed to filtered air under identical conditions.

On days 10 and 21 after the initial cigarette exposure, mice in the AAV9-Foxp1 group received intratracheal injection of AAV9 particles (1.0×10^{10} viral genomes in 60 µL saline, lc-bio, Hangzhou, China) expressing Foxp1, as previously described [11]. This strategy was used to ensure effective expression and sustained activity of Foxp1 during the critical period of model establishment. Mice in the AAV9-vector group were administered an equal dose of empty AAV9-vectors as controls.

All mice were then euthanized through intraperitoneal injection of an overdose of sodium pentobarbital (150 mg/kg, P3761, Sigma-Aldrich, St. Louis, MO, USA). Finally, lung tissues were collected for subsequent molecular and histological analyses.

Hematoxylin and Eosin (H&E) Staining

Lung tissues from mice were embedded in paraffin and then sectioned into 5-µm slices. Tissue sections were deparaffinized in xylene, rehydrated through gradient ethanol (100%, 90%, 80%, and 70%), washed with distilled water, and stained with hematoxylin and eosin using the H&E staining kit (BA4025, Baso, Zhuhai, China). After staining, the slices were dehydrated with gradient ethanol (70%, 80%, 95%, and 100%), cleared with xylene, mounted with neutral balsam (I1711, Bioswamp, Wuhan, China), and observed under a microscope (NIB910, minghuikj, Guangzhou, China). As previously described [7], the mean linear intercept (MLI) was determined by selecting regions devoid of airways and blood vessels and counting the number of intersections of virtual lines of known length with alveolar septa. The MLI was calculated by dividing the total line length by the number of interceptions, with increased MLI indicating alveolar enlargement.

Immunofluorescence Staining

After conventional dewaxing and rehydration, the paraffin-embedded slices were subjected to antigen retrieval in ethylenediaminetetraacetic acid (EDTA) buffer (pH 9.0, BL617A, Biosharp, China) using a microwave. Subsequently, the sections were fixed in 4% paraformaldehyde (BL539A, Biosharp, Hefei, China) and blocked with blocking buffer (BL736A, Biosharp, China) for 1 hour. After washing with phosphate-buffered saline (PBS, SNB-001, Sunncell, Wuhan, China), the sections were incubated with primary antibody CD31 (1:200, 14-0311-82, ThermoFisher, Waltham, MA, USA). Then, secondary antibody Goat anti-Rat IgG (A-21434, 1 µg/mL, ThermoFisher, Waltham, MA, USA), Terminal deoxynucleotidyl transferase-mediated deoxyuridine triphosphate (dUTP) nick end labeling (TUNEL, FITC, BL645A, Biosharp, Hefei, China) and 4',6-Diamidino-2'-phenylindole (DAPI) (BL120A, Biosharp, Hefei, China) were applied to label apoptotic nuclei and total nuclei, respectively. Finally, fluorescence signals were observed using a fluorescence microscope (BZ-X800E, KEYENCE, Shanghai, China). The relative $CD31^+TUNEL^+$ area (%) was calculated as follows: $CD31^+TUNEL^+$ area (%) = (Area_$CD31^+TUNEL^+$ / Total_Area) × 100%.

Cell Culture and Transfection

Human pulmonary microvascular endothelial cells (hPMVECs, IMP-H037, Immocell, Xiamen, China) were cultured in hPMVECs-specific medium (IMP-H037-1, Immocell, Xiamen, China) and incubated at 37 °C in humidified conditions with 5% CO_2. Cell identity was confirmed by STR profiling, and cultures were confirmed to be free of mycoplasma contamination. *Foxp1* and *MMP9* overexpression plasmids (oe-Foxp1/oe-MMP9; G107468/G115084) and their corresponding negative control (NC; pDONR223 vector) were obtained from Youbio (Changsha, China). Se-

quence details for Foxp1, MMP9, and the pDONR223 vector are given in **Supplementary File 1**. Cells were seeded into six-well plates at a density of approximately 5×10^5 cells per well one day before transfection. Opti-MEM Medium (31985062; ThermoFisher, Waltham, MA, USA) was employed to dilute the transfection reagents and plasmids. After thorough blending, the plasmid-lipid complexes were added to the six-well plates and incubated for 48 hours. Finally, transfection efficiency was assessed using quantitative reverse transcription polymerase chain reaction (qRT-PCR).

Table 1. A list of primers and their sequences used in this study.

Gene	5′–> 3′
Foxp1 (human) Forward	GCAGTGTGCGAAGATTTCCAA
Foxp1 (human) Reverse	TCACATGCAGGTGGGTCATC
MMP9 (human) Forward	GCCACTACTGTGCCTTTGAGTC
MMP9 (human) Reverse	CCCTCAGAGAATCGCCAGTACT
GAPDH (human) Forward	CGACAGCAGCCGCATCTT
GAPDH (human) Reverse	CCAATACGACCAAATCCGTTG

Foxp1, forkhead box protein 1; *MMP9*, matrix metalloproteinase 9; *GAPDH*, glyceraldehyde-3-phosphate dehydrogenase.

Cell Grouping

The cellular experiments were divided into two parts. In the first part, cells were divided into four groups: control, CSE, NC, and Foxp1. Cells in the control group were incubated under normal culture conditions, whereas the other three groups were exposed to 2% CSE. However, cells in the NC and Foxp1 groups were transfected with NC or oe-Foxp1 for 48 hours before CSE exposure.

CSE was prepared as previously described with slight modifications [7]. Briefly, smoke from five cigarettes (Daqianmen, China), each containing 11 mg tar and 0.8 mg nicotine, was bubbled through 10 mL of hPMVECs-specific medium. The resulting medium was filtered through a 0.22 µm filter, designated as 100% CSE, and then diluted to 2% using fresh hPMVEC medium before use.

In the second part, cells were divided into four groups: CSE+NC, Foxp1, Foxp1+NC, and Foxp1+MMP9. All these four groups were exposed to 2% CSE; however, cells were first transfected with NC, oe-Foxp1, or co-transfected with oe-Foxp1 and NC/oe-MMP9, as appropriate, before CSE exposure.

Relative Gene Expression Analysis

Total RNA was isolated from the cells using TRIzol reagent (PMK0833; BIOPRIMACY, Wuhan, China), and complementary DNA (cDNA) was synthesized using a reverse transcription kit (PMK0832, BIOPRIMACY, Wuhan, China). Thereafter, qPCR was conducted on a Real-Time PCR System (RTQ-960, Acon, Hangzhou, China) using qPCR MasterMix (Q411-02, Vazyme, Nanjing, China). Gene expression levels were normalized to Glyceraldehyde-3-phosphate dehydrogenase (GAPDH) and relative expression was calculated using the $2^{-\Delta\Delta CT}$ method. Primers used in qPCR are listed in Table 1.

Western Blot Analysis

Total proteins were isolated from tissues and cells using RIPA buffer (PMK0213, BIOPRIMACY, Wuhan, China) and quantified using a BCA kit (PMK0442, BIOPRIMACY, Wuhan, China). Proteins were resolved by SDS-PAGE (PH0331, PHYGENE, Fuzhou, China), and then transferred onto nitrocellulose membranes. After being blocked with Western blocking buffer (BL535A, Biosharp, Hefei, China), membranes underwent overnight incubation at 4 °C with protein-specific primary antibodies (Table 2). The following day, membranes were washed and incubated with corresponding secondary antibodies (Table 2) for 1 hour at room temperature. Protein bands were visualized using an imaging system (JY04S-3, Beijing JUNYI Electrophoresis Co., Ltd., Beijing, China) with ECL Kit (BL520A, Biosharp, Hefei, China). Relative protein expression was determined as the ratio of the gray value of the target protein to that of the internal reference protein. GAPDH levels were normalized to the mean value of the Con or CSE+NC group.

Cell Viability and Apoptosis

Cell viability was evaluated using the cell counting kit-8 (CCK-8, PH1759, PHYGENE, Fuzhou, China). Briefly, cells were inoculated in 96-well plates and then received the indicated treatments. CCK-8 reagent was then added to each well, and the plates were incubated for 2 hours at 37 °C. OD was measured at 450 nm using a microplate reader (HBS-ScanX, DeTiebio, China). Relative cell viability (%) was calculated as follows: Relative cell viability (%) = $(OD_{experiment} - OD_{blank}) / (OD_{control} - OD_{blank}) \times 100\%$. Cellular apoptosis was assessed using the Annexin V-FITC/PI Apoptosis Detection Kit (C9102, Warbio, Nanjing, China). Cells were re-suspended in the binding buffer and then stained with Annexin V-FITC and PI in the dark. After washing with PBS, the apoptotic rate was evaluated using a flow cytometer (Attune CytPix, ThermoFisher, Waltham, MA, USA).

Assessment of Endothelial Permeability

Endothelial permeability was determined as previously described [12]. In short, cells were cultured in the Transwell inserts and then received the indicated treatments. FITC-dextran (FD40, Merck, Darmstadt, Germany) was added to the upper chamber of the inserts and incubated for 1 hour. After that, the fluorescence intensity of FITC in the lower chamber was then assessed using a luminometer (SpectraMax Gemini EM, MD, Shenzhen, China) with an excitation wavelength of 490 nm and an emission wavelength of 530 nm.

Table 2. Primary and secondary antibodies used in Western blotting.

Antibody	Catalog	Molecular weight	Dilution	Manufacturer
Anti-SDC-1	ab128936	32 kDa	1/1000	Abcam, UK
Anti-Foxp1	ab134055	75 kDa	1/1000	Abcam, UK
Anti-MMP9	ab283575	78 kDa	1/1000	Abcam, UK
Anti-VCAN	ab270445	373 kDa	1/1000	Abcam, UK
Anti-GAPDH	#2118	37 kDa	1/1000	CST, USA
Goat anti rabbit	ab205718	—	1/2000	Abcam, UK

SDC-1, syndecan-1; VCAN, versican.

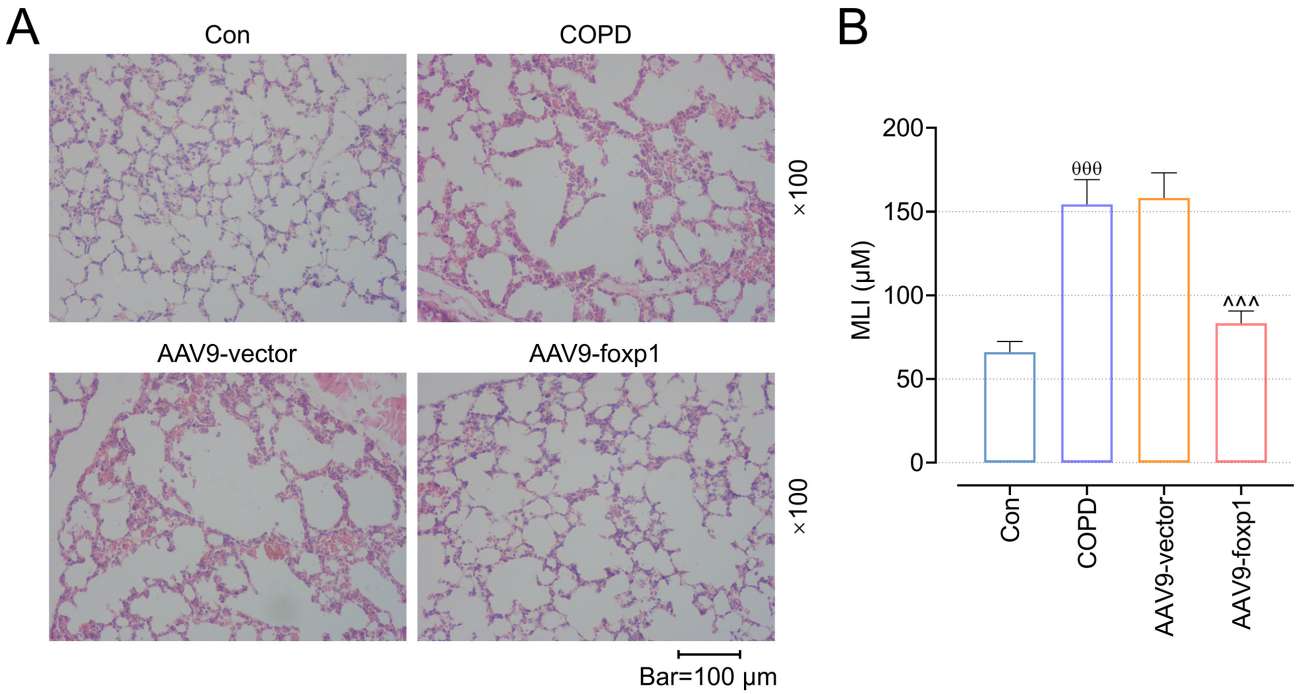

Fig. 1. Effects of AAV9-Foxp1 on lung tissue lesion in COPD mice. Male C57BL/6J mice administered with AAV9-vector AAV9-foxp1 were exposed to cigarette smoke to establish the COPD model. (A,B) The lung tissue injuries among all four groups of mice were assessed using H&E staining (magnification, 100×). Bar: 100 μm. Alveolar size was measured by mean linear intercept (MLI) (n = 6). $^{\theta\theta\theta}p < 0.001$ vs. the control group. $^{\wedge\wedge\wedge}p < 0.001$ vs. the AAV9-Vector group. Data were presented as mean ± standard deviation from at least three independent experiments. AAV, adeno-associated virus; COPD, chronic obstructive pulmonary disease; H&E, hematoxylin and eosin; NC, negative control; Foxp1, forkhead box protein 1.

Tube Formation Assay

Treated cells were seeded into 96-well plates pre-coated with 100 μL of Matrigel (356231, Corning, Midland, MI, USA) and incubated at 37 °C for 5 hours. Tube formation was visualized using a microscope, and the total tube length was measured with ImageJ software (v1.6.0, ImageJ Software Inc., Bethesda, MA, USA).

Statistical Analyses

Statistical analysis was performed using GraphPad Prism v8.0 (GraphPad software, La Jolla, CA, USA). Data were represented as mean ± standard deviation. Multiple-group comparisons were conducted using one-way analysis of variance (ANOVA) followed by Tukey's post hoc test. A p-value of <0.05 was considered statistically significant.

Results

AAV9-Foxp1 Ameliorates the Increase in MLI and Endothelial Apoptosis, Regulates MMP9 and Glycocalyx-Associated Protein Levels in COPD Mice

To investigate the role of *Foxp1* in COPD, we first evaluated its function in an *in vivo* model. H&E staining demonstrated that the MLI in the lung tissue of cigarette smoke-exposed mice was significantly increased compared to the control mice, indicating the induction of emphysematous alterations (Fig. 1A,B, $p < 0.05$). Furthermore, CD31 and TUNEL double fluorescence staining revealed a substantial increase in endothelial cell apoptosis in the lung tissue of COPD mice (Fig. 2A,B, $p < 0.05$). However, both the increased MLI and the number of apoptotic endothelial

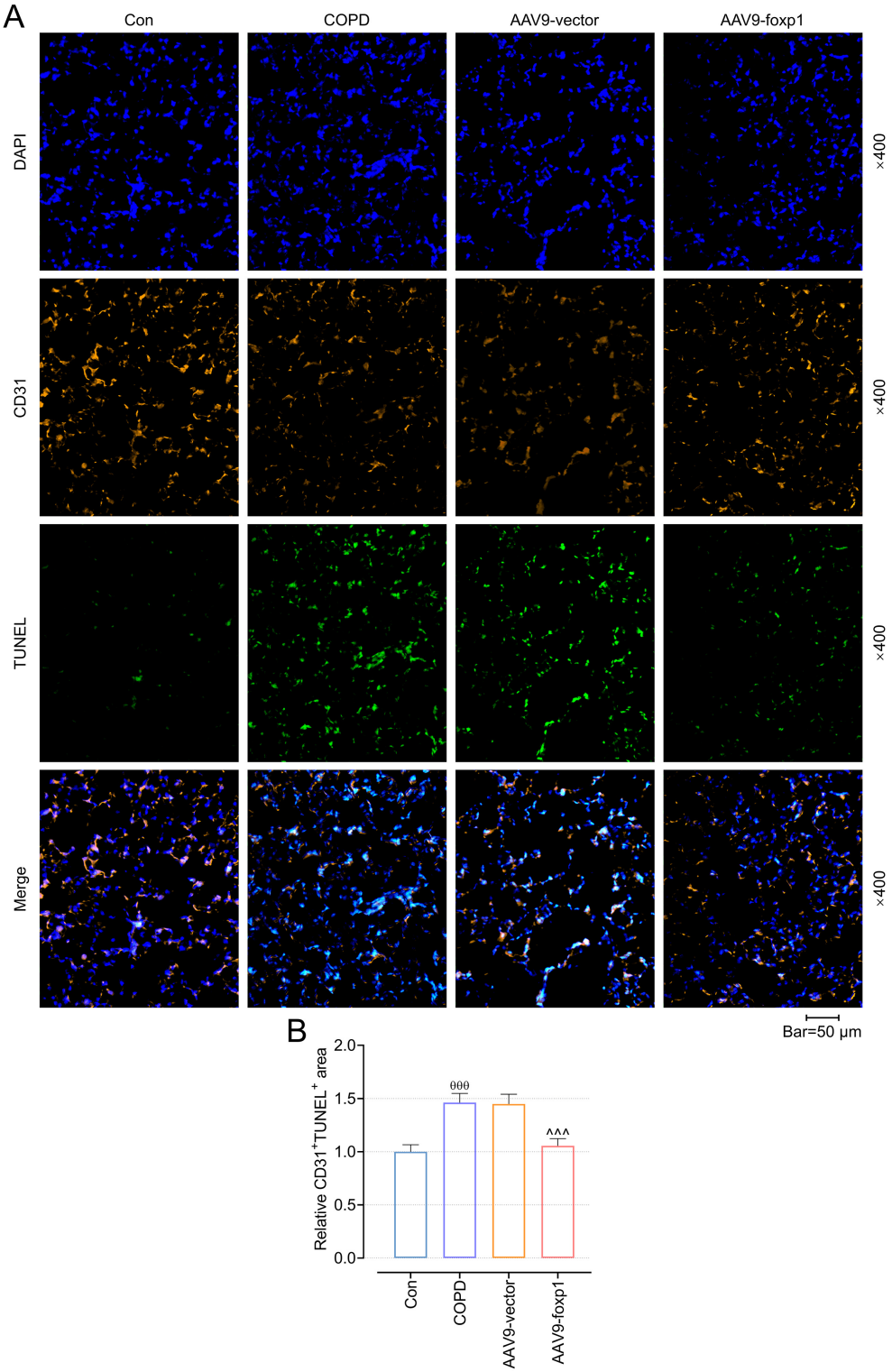

Fig. 2. AAV9-Foxp1 inhibits apoptosis in PMVECs among COPD mice. Male C57BL/6J mice administered with AAV9-vector or AAV9-foxp1 were exposed to cigarette smoke to establish the COPD model. (A,B) An immunofluorescence assay was used to detect the apoptotic PMVECs. Blue represents nuclear staining with DAPI. Gold indicates endothelial cells stained with CD31. Green represents apoptotic cells stained with TUNEL (magnification, 400×). Bar: 50 μm. $^{\theta\theta\theta}p < 0.001$ vs. the control group. $^{\wedge\wedge\wedge}p < 0.001$ vs. the AAV9-Vector group. Data were presented as mean ± standard deviation from at least three independent experiments. TUNEL, terminal deoxynucleotidyl transferase-mediated deoxyuridine triphosphate nick end labeling; PMVECs, pulmonary microvascular endothelial cells.

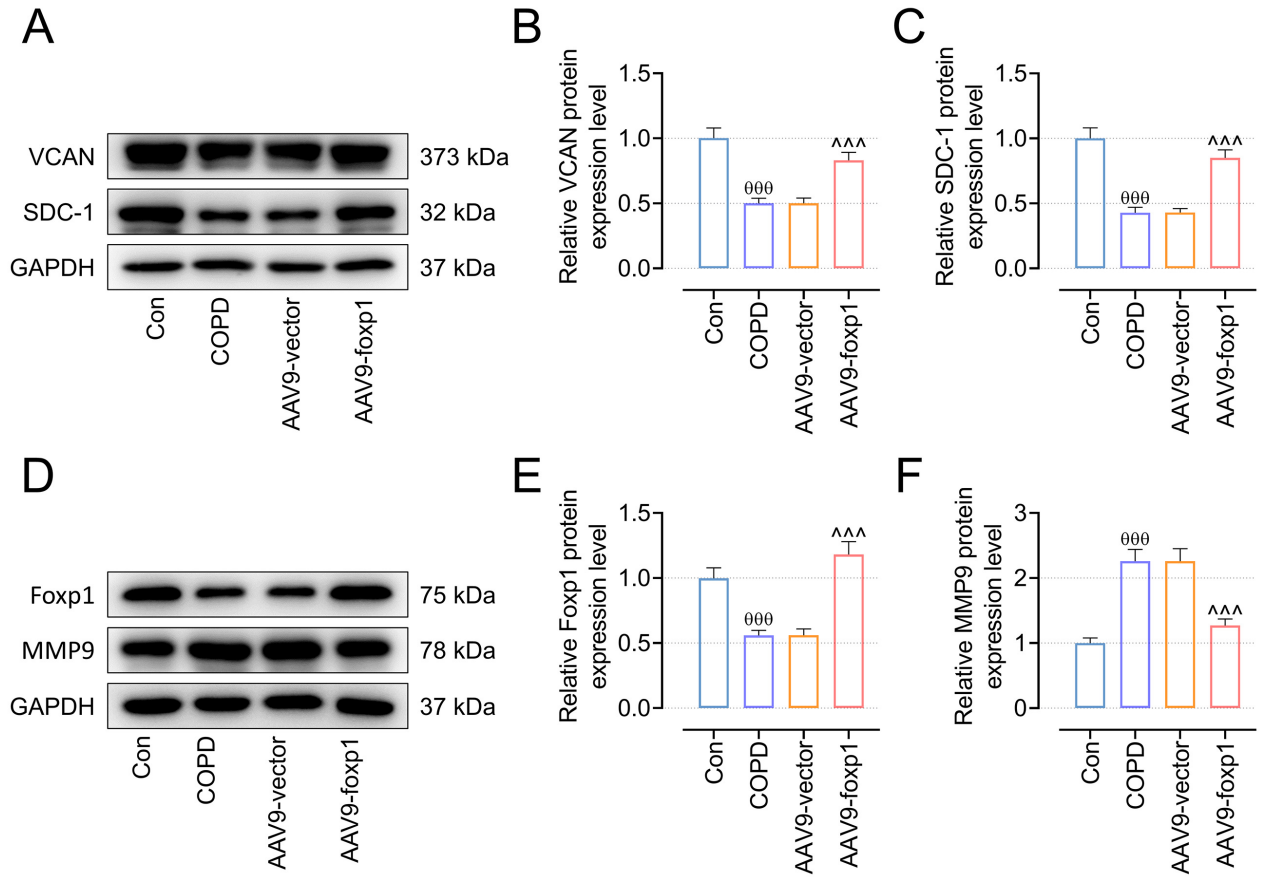

Fig. 3. AAV9-Foxp1 suppresses MMP9 expression and promotes the expression of VCAN, SDC-1 and Foxp1 in the lung tissue of COPD mice. Male C57BL/6J mice administered with AAV9-vector or AAV9-Foxp1 were exposed to cigarette smoke to establish the COPD model. (A–C) The expressions of glycocalyx-related proteins (VCAN and SDC-1) were determined using Western blotting. GAPDH served as an internal control. (D–F) The expressions of Foxp1 and MMP9 were determined using Western blotting. GAPDH served as an internal control. $^{\theta\theta\theta}p < 0.001$ vs. the control group. $^{\wedge\wedge\wedge}p < 0.001$ vs. the AAV9-Vector group. Data were presented as mean ± standard deviation from at least three independent experiments.

cells in the lung tissue of COPD mice were effectively reduced after AAV9-Foxp1 treatment (Fig. 1A,B and Fig. 2, $p < 0.05$).

Additionally, Western blotting revealed that the expression of Foxp1 and glycocalyx-associated proteins (VCAN and syndecan-1 (SDC-1)) was decreased in the lung tissue of cigarette smoke-exposed mice, whereas MMP9 expression was increased (Fig. 3A–F, $p < 0.05$). However, treatment with AAV9-Foxp1 effectively restored the expression of VCAN, SDC-1, and Foxp1, while attenuating MMP9 levels (Fig. 3A–F, $p < 0.05$).

Foxp1 Overexpression Ameliorates CSE-induced Functional Impairment of hPMVECs and Regulates Glycocalyx Stability in a MMP9-Dependent Manner

To further investigate the role of *Foxp1* in COPD, we performed *in vitro* experiments using hPMVECs and first confirmed efficient transfection of oe-Foxp1 (Fig. 4A, $p < 0.05$). Exposure to CSE substantially decreased cell viability (Fig. 4B, $p < 0.05$), increased apoptosis (Fig. 4C,D, $p < 0.05$), enhanced endothelial cell permeability (Fig. 4E, $p < 0.05$), and diminished relative tube length (Fig. 4F,G, $p < 0.05$). All these changes were effectively reversed by oe-Foxp1 treatment (Fig. 4B–G, $p < 0.05$). At the molecular level, CSE downregulated Foxp1 and SDC-1 and upregulated MMP9 in hPMVECs (Fig. 4H,I, $p < 0.05$), which were reversed upon oe-Foxp1 treatment (Fig. 4H,I, $p < 0.05$).

First, successful transfection was confirmed through increased *MMP9* expression in the MMP9 group (Fig. 5A, $p < 0.05$). Then, to determine whether the protective effects of oe-Foxp1 in CSE-treated hPMVECs are attributed to MMP9 suppression, we co-overexpressed MMP9 and Foxp1 in these cells. Notably, MMP9 counteracted the protective effects of Foxp1 on cell viability (Fig. 5B, $p < 0.05$), apoptosis (Fig. 5C,D, $p < 0.05$), endothelial permeability (Fig. 5E, $p < 0.05$), and tube formation ability (Fig. 5F,G, $p < 0.05$). Furthermore, co-expression of MMP9 significantly reversed the oe-Foxp1-induced downregulation of MMP9 and upregulation of SDC-1 (Fig. 5H,I, $p < 0.05$).

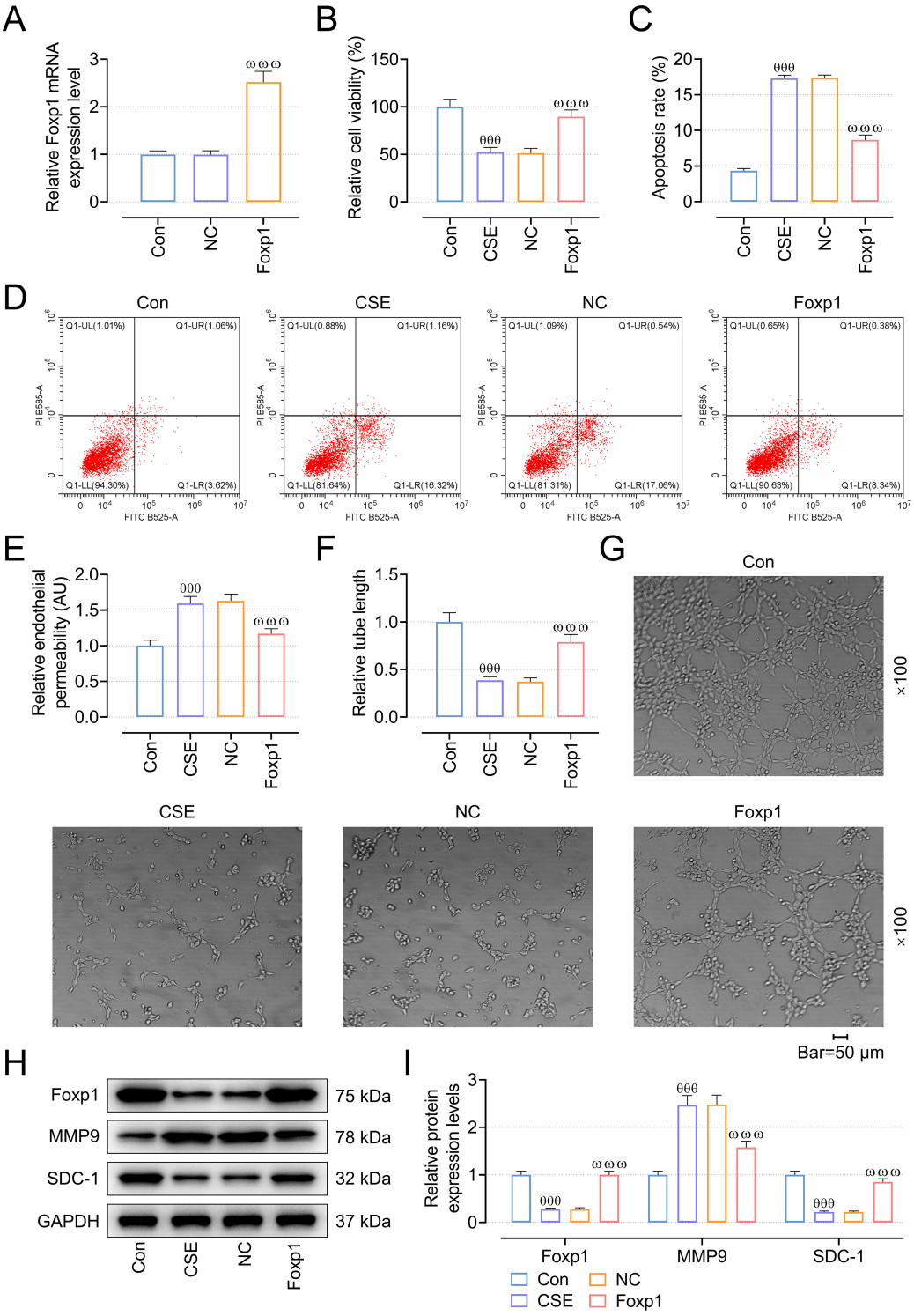

Fig. 4. Effects of Foxp1 overexpression on CSE-treated hPMVECs. (A) The transfection efficiency of the Foxp1 overexpression plasmid was determined using qRT-PCR. *GAPDH* served as an internal control. (B) The viability of hPMVECs in all four groups was determined using the CCK-8 assay. (C,D) The apoptosis of hPMVECs in all four groups was determined using flow cytometry. (E) The endothelial permeability was examined through dextran-conjugated FITC. (F,G) The tube formation ability of hPMVECs in all four groups was determined through the tube formation assay (magnification, 100×). Bar: 50 μm. (H,I) The expressions of Foxp1, MMP9, and SDC-1 were assessed using Western blotting. GAPDH served as an internal control. $^{\theta\theta\theta}p < 0.001$ vs. the control group. $^{\omega\omega\omega}p < 0.001$ vs. the NC group. Data were presented as mean ± standard deviation from at least three independent experiments. hPMVECs, human pulmonary microvascular endothelial cells; CSE, cigarette smoke extract; qRT-PCR, quantitative reverse transcription polymerase chain reaction; CCK-8, cell counting kit-8.

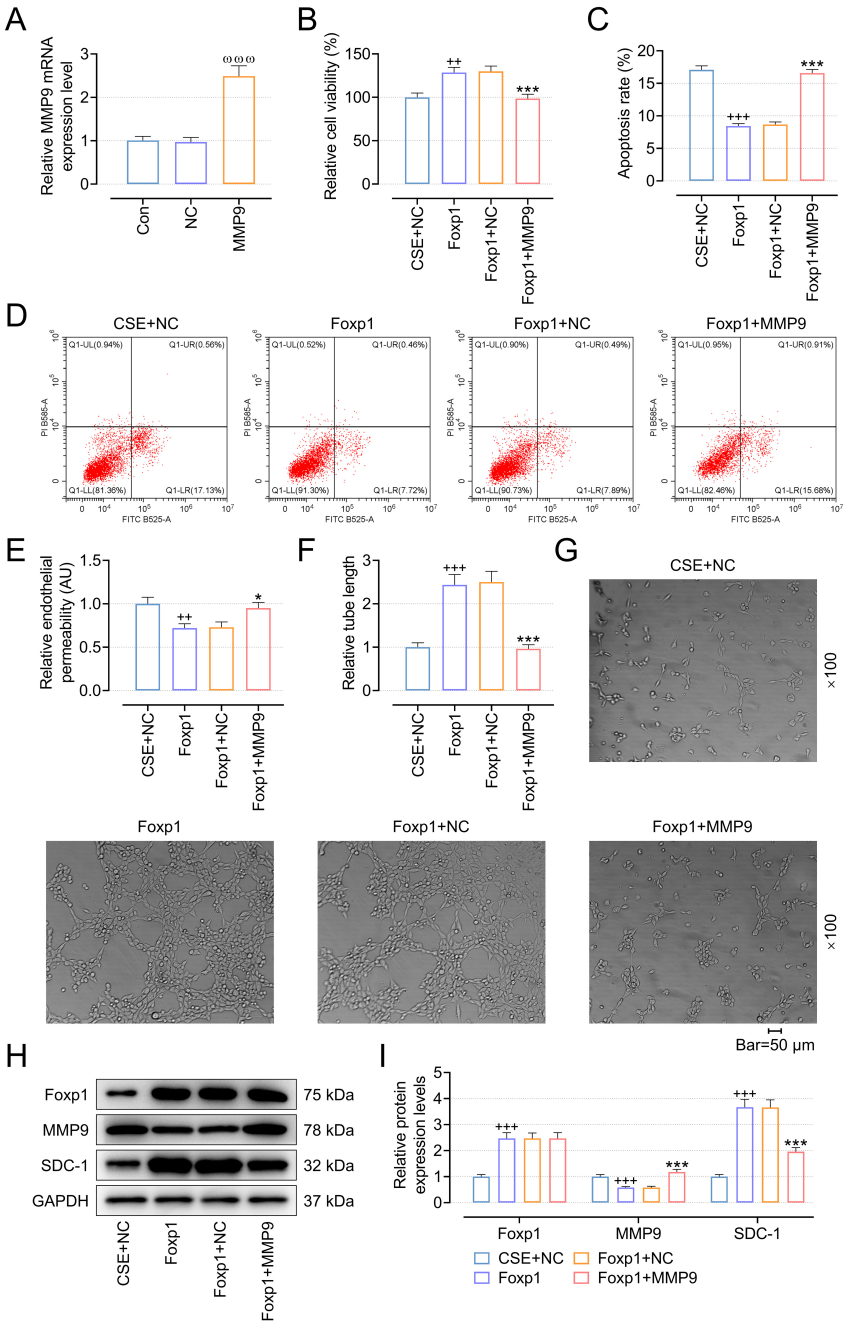

Fig. 5. MMP9 overexpression reverses the effects of Foxp1 overexpression on CSE-treated hPMVECs. (A) The transfection efficiency of the MMP9 overexpression plasmid was determined using qRT-PCR. *GAPDH* served as internal control. (B) The viability of hPMVECs in all four groups was determined using the CCK-8 assay. (C,D) Apoptosis of hPMVECs in all four groups was evaluated using flow cytometry. (E) The endothelial permeability was examined through dextran-conjugated FITC. (F,G) The tube formation ability of hPMVECs in all four groups was determined through the tube formation assay (magnification, 100×). Bar: 50 μm. (H,I) The expressions of Foxp1, MMP9 and SDC-1 were determined using Western blotting. GAPDH served as an internal control. $^{\omega\omega\omega}p < 0.001$ vs. the NC group. $^{++}p < 0.01$, $^{+++}p < 0.001$ vs. the shNC group. $^{*}p < 0.05$, $^{***}p < 0.001$ vs. the Foxp1+NC group. Data were presented as mean ± standard deviation from at least three independent experiments.

Discussion

This study emphasizes the crucial role of pulmonary microvascular endothelial cells (PMVECs) in COPD pathogenesis. It reveals that Foxp1 can improve COPD by preventing endothelial glycocalyx injury and reducing PMVECs apoptosis, suggesting a promising therapeutic target for managing COPD.

Cigarette smoke is a well-established risk factor for COPD; hence, we established a COPD model by expos-

ing mice to cigarette smoke, a widely accepted approach [13]. Increased apoptosis of endothelial cells in COPD patients causes significant lung tissue destruction and emphysema development, and cigarette smoke has been shown to induce apoptosis in PMVECs [14]. Therefore, preventing apoptosis in PMVECs has emerged as a promising strategy for the prevention and treatment of COPD. In our study, COPD mice treated with AAV9-Foxp1 showed reduced MLI and decreased endothelial apoptosis compared to untreated COPD mice, whereas oe-Foxp1 effectively reversed CSE-induced apoptosis of hPMVECs *in vitro*. Low Foxp1 expression has been linked to airflow obstruction and emphysema [15], and Foxp1 has been reported to cooperate with histone deacetylase 2 to regulate lung epithelial injury [16]. Collectively, these observations facilitate a protective role of Foxp1 in alleviating cigarette smoke-induced emphysema and endothelial cell apoptosis.

Besides promoting endothelial cell apoptosis, cigarette smoke impairs endothelial cell angiogenesis and increases endothelial permeability [17,18]. A growing body of evidence suggests that disrupted angiogenesis hinders lung repair in COPD patients and increases the incidence of hypoxemia and pulmonary hypertension [19]. Foxp1 has been widely reported to stimulate angiogenesis; for example, Dinghui Wang *et al.* [20] reported that Foxp1 enhances endothelial cell proliferation and tube formation in adult rats after myocardial infarction, underscoring its potential as a therapeutic target for cardiac angiogenesis. In contrast, the absence of Foxp1 decreases neovascularization [21]. On the other hand, increased endothelial cell permeability induced by cigarette smoke also promotes emphysema progression [18]. However, the role of Foxp1 in modulating PMVECs permeability has not been previously investigated. In this study, we found that oe-Foxp1 increased cell viability and tube-forming capability while reducing endothelial permeability in CSE-exposed hPMVECs, suggesting a potential supportive role in endothelial function. However, further investigation is required to fully establish its pro-angiogenic effects in the context of COPD.

Our study focuses on the regulatory effect of Foxp1 on the endothelial glycocalyx. As a key component of the endothelial barrier, the glycocalyx modulates vascular permeability and protects endothelial cells, making it a potential therapeutic target for various diseases [22]. SDC-1 and VCAN, key components of glycocalyx, show reduced expression in the distal lung parenchyma [23] and serum [24] of patients with COPD. Previous research has reported that miR-143 induces endothelial injury by targeting SDCs and VCAN [25]. Overall, these results suggest that reduced SDC-1 and VCAN levels in the glycocalyx may contribute to endothelial injury and the pathogenesis of COPD.

In our study, Foxp1 reversed the CSE-induced downregulation of SDC-1 and VCAN expression, indicating that Foxp1 may protect endothelial cells by maintaining the stability of glycocalyx. More importantly, this protective effect underscores Foxp1 as a promising therapeutic target for COPD, suggesting that strategies aimed at enhancing its expression or activity could help preserve endothelial barrier function and mitigate disease progression. Additionally, previous studies have reported that MMP9 is involved in the degradation of SDC-1 and VCAN, thereby promoting pulmonary edema [9,26]. Conversely, Foxp1 can support endothelial repair by reducing MMP9 expression [8]. Consistently, we found that the impact of Foxp1 on hPMVECs viability, tube formation, apoptosis, endothelial permeability, and glycocalyx-related protein expression was all reversed by oe-MMP9, indicating that Foxp1 prevents endothelial cell injury primarily by inhibiting MMP9 expression.

Collectively, these findings demonstrate a novel mechanism by which Foxp1 protects against COPD-associated endothelial dysfunction, preserving glycocalyx integrity via MMP9 inhibition, and offer valuable insights for developing targeted therapies for COPD.

Conclusion

In conclusion, this study reports for the first time that the Foxp1/MMP9 axis plays a crucial role in COPD progression by regulating endothelial glycocalyx integrity and hPMVECs apoptosis. These findings underscore the potential for targeting Foxp1 as a therapeutic approach for COPD, indicating that the Foxp1 agonists could be developed to maintain endothelial function and alleviate disease progression.

Availability of Data and Materials

The analyzed data sets generated during the study are available from the corresponding author on reasonable request.

Author Contributions

FZ and XLH designed the research study. YW and YS performed the research. FZ and YW collected and analyzed the data. XLH and YS has been involved in drafting the manuscript and all authors have been involved in revising it critically for important intellectual content. All authors give final approval of the version to be published. All authors have participated sufficiently in the work to take public responsibility for appropriate portions of the content and agreed to be accountable for all aspects of the work in ensuring that questions related to its accuracy or integrity.

Ethics Approval and Consent to Participate

All animal-related experimental protocols were approved by the Institutional Animal Care and Use Committee, Zhejiang Center of Laboratory Animals (ZJCA) (ZJCLA-IACUC-20011026).

Acknowledgment

Not applicable.

Funding

This research received no external funding.

Conflict of Interest

The authors declare no conflict of interest.

Supplementary Material

Supplementary material associated with this article can be found, in the online version, at https://doi.org/10.24976/Discov.Med.202537201.200.

References

[1] Vogelmeier CF, Román-Rodríguez M, Singh D, Han MK, Rodríguez-Roisin R, Ferguson GT. Goals of COPD treatment: Focus on symptoms and exacerbations. Respiratory Medicine. 2020; 166: 105938. https://doi.org/10.1016/j.rmed.2020.105938.

[2] Rabe KF, Hurd S, Anzueto A, Barnes PJ, Buist SA, Calverley P, *et al*. Global strategy for the diagnosis, management, and prevention of chronic obstructive pulmonary disease: GOLD executive summary. American Journal of Respiratory and Critical Care Medicine. 2007; 176: 532–555. https://doi.org/10.1164/rccm.200703-456SO.

[3] Sandelowsky H, Weinreich UM, Aarli BB, Sundh J, Høines K, Stratelis G, *et al*. COPD - do the right thing. BMC Family Practice. 2021; 22: 244. https://doi.org/10.1186/s12875-021-01583-w.

[4] Hisata S, Racanelli AC, Kermani P, Schreiner R, Houghton S, Palikuqi B, *et al*. Reversal of emphysema by restoration of pulmonary endothelial cells. The Journal of Experimental Medicine. 2021; 218: e20200938. https://doi.org/10.1084/jem.20200938.

[5] Butler PJ, Bhatnagar A. Mechanobiology of the abluminal glycocalyx. Biorheology. 2019; 56: 101–112. https://doi.org/10.3233/BIR-190212.

[6] Mitra R, Nersesyan A, Pentland K, Melin MM, Levy RM, Ebong EE. Diosmin and its glycocalyx restorative and anti-inflammatory effects on injured blood vessels. FASEB Journal. 2022; 36: e22630. https://doi.org/10.1096/fj.202200053RR.

[7] Jiang T, Hu W, Zhang S, Ren C, Lin S, Zhou Z, *et al*. Fibroblast growth factor 10 attenuates chronic obstructive pulmonary disease by protecting against glycocalyx impairment and endothelial apoptosis. Respiratory Research. 2022; 23: 269. https://doi.org/10.1186/s12931-022-02193-5.

[8] Chen X, Xu J, Bao W, Li H, Wu W, Liu J, *et al*. Endothelial Foxp1 Regulates Neointimal Hyperplasia Via Matrix Metalloproteinase-9/Cyclin Dependent Kinase Inhibitor 1B Signal Pathway. Journal of the American Heart Association. 2022; 11: e026378. https://doi.org/10.1161/JAHA.122.026378.

[9] Zhang D, Zhang JT, Pan Y, Liu XF, Xu JW, Cui WJ, *et al*. Syndecan-1 Shedding by Matrix Metalloproteinase-9 Signaling Regulates Alveolar Epithelial Tight Junction in Lipopolysaccharide-Induced Early Acute Lung Injury. Journal of Inflammation Research. 2021; 14: 5801–5816. https://doi.org/10.2147/JIR.S331020.

[10] Andreas A, Maloy A, Nyunoya T, Zhang Y, Chandra D. The FoxP1 gene regulates lung function, production of matrix metalloproteinases and inflammatory mediators, and viability of lung epithelia. Respiratory Research. 2022; 23: 281. https://doi.org/10.1186/s12931-022-02213-4.

[11] Guan R, Yuan L, Li J, Wang J, Li Z, Cai Z, *et al*. Bone morphogenetic protein 4 inhibits pulmonary fibrosis by modulating cellular senescence and mitophagy in lung fibroblasts. The European Respiratory Journal. 2022; 60: 2102307. https://doi.org/10.1183/13993003.02307-2021.

[12] Guo X, Lin Y, Lin Y, Zhong Y, Yu H, Huang Y, *et al*. PM2.5 induces pulmonary microvascular injury in COPD via METTL16-mediated m6A modification. Environmental Pollution. 2022; 303: 119115. https://doi.org/10.1016/j.envpol.2022.119115.

[13] Fricker M, Deane A, Hansbro PM. Animal models of chronic obstructive pulmonary disease. Expert Opinion on Drug Discovery. 2014; 9: 629–645. https://doi.org/10.1517/17460441.2014.909805.

[14] Song Q, Chen P, Liu XM. The role of cigarette smoke-induced pulmonary vascular endothelial cell apoptosis in COPD. Respiratory Research. 2021; 22: 39. https://doi.org/10.1186/s12931-021-01630-1.

[15] Bahr TM, Hughes GJ, Armstrong M, Reisdorph R, Coldren CD, Edwards MG, *et al*. Peripheral blood mononuclear cell gene expression in chronic obstructive pulmonary disease. American Journal of Respiratory Cell and Molecular Biology. 2013; 49: 316–323. https://doi.org/10.1165/rcmb.2012-0230OC.

[16] Chokas AL, Trivedi CM, Lu MM, Tucker PW, Li S, Epstein JA, *et al*. Foxp1/2/4-NuRD interactions regulate gene expression and epithelial injury response in the lung via regulation of interleukin-6. The Journal of Biological Chemistry. 2010; 285: 13304–13313. https://doi.org/10.1074/jbc.M109.088468.

[17] Lu Q, Gottlieb E, Rounds S. Effects of cigarette smoke on pulmonary endothelial cells. American Journal of Physiology. Lung Cellular and Molecular Physiology. 2018; 314: L743–L756. https://doi.org/10.1152/ajplung.00373.2017.

[18] Rounds S, Lu Q. Cigarette smoke alters lung vascular permeability and endothelial barrier function (2017 Grover Conference Series). Pulmonary Circulation. 2018; 8: 2045894018794000. https://doi.org/10.1177/2045894018794000.

[19] Su Y, Cao W, Han Z, Block ER. Cigarette smoke extract inhibits angiogenesis of pulmonary artery endothelial cells: the role of calpain. American Journal of Physiology. Lung Cellular and Molecular Physiology. 2004; 287: L794–800. https://doi.org/10.1152/ajplung.00079.2004.

[20] Wang D, Liu B, Xiong T, Yu W, Yang H, Wang J, *et al*. Transcription factor Foxp1 stimulates angiogenesis in adult rats after myocardial infarction. Cell Death Discovery. 2022; 8: 381. https://doi.org/10.1038/s41420-022-01180-5.

[21] Grundmann S, Lindmayer C, Hans FP, Hoefer I, Helbing T, Pasterkamp G, *et al*. FoxP1 stimulates angiogenesis by repressing the inhibitory guidance protein semaphorin 5B in endothelial cells. PLoS ONE. 2013; 8: e70873. https://doi.org/10.1371/journal.pone.0070873.

[22] Cao RN, Tang L, Xia ZY, Xia R. Endothelial glycocalyx as a potential theriapeutic target in organ injuries. Chinese Medical Journal. 2019; 132: 963–975. https://doi.org/10.1097/CM9.0000000000000177.

[23] Annoni R, Lanças T, Yukimatsu Tanigawa R, de Medeiros Matsushita M, de Morais Fernezlian S, Bruno A, *et al*. Extracellular matrix composition in COPD. The European Respiratory Journal. 2012; 40: 1362–1373. https://doi.org/10.1183/09031936.00192611.

[24] Li D, Wu Y, Guo S, Qin J, Feng M, An Y, *et al*. Circulating syndecan-1 as a novel biomarker relates to lung function, systemic inflammation, and exacerbation in COPD. International

Journal of Chronic Obstructive Pulmonary Disease. 2019; 14: 1933–1941. https://doi.org/10.2147/COPD.S207855.

[25] Müller-Deile J, Gellrich F, Schenk H, Schroder P, Nyström J, Lorenzen J, *et al*. Overexpression of TGF-β Inducible microRNA-143 in Zebrafish Leads to Impairment of the Glomerular Filtration Barrier by Targeting Proteoglycans. Cellular Physiology and Biochemistry. 2016; 40: 819–830. https://doi.org/10.1159/000453142.

[26] Passi A, Negrini D, Albertini R, Miserocchi G, De Luca G. The sensitivity of versican from rabbit lung to gelatinase A (MMP-2) and B (MMP-9) and its involvement in the development of hydraulic lung edema. FEBS Letters. 1999; 456: 93–96. https://doi.org/10.1016/s0014-5793(99)00929-1.